



# Spatial Analysis of Groundwater Potential Using GIS Based Multi Criteria Decision Analysis Method in Lake Tana Basin, Ethiopia

Agumase T. Kindie<sup>1,2(✉)</sup>, Temesegen Enku<sup>2</sup>, Mamaru A. Moges<sup>2</sup>, Berhanu S. Geremew<sup>1,2</sup>, and Haimanot B. Atinkut<sup>3</sup>

<sup>1</sup> Department of Hydraulic and Water Resource Engineering,  
Gondar Institute of Technology, University of Gondar,  
P.O. Box 196, Gondar, Ethiopia  
agumasekt2006@gmail.com

<sup>2</sup> Department of Hydraulic and Water Resource, Engineering,  
Faculty of Civil and Water Resource Engineering, Bahir Dar University,  
P.O. Box 79, Bahir Dar, Ethiopia

<sup>3</sup> Colleges of Agriculture and Rural Transformation, University of Gondar,  
P.O. Box 196, Gondar, Ethiopia

**Abstract.** Groundwater resource development for various uses is increasing in the Lake Tana basin, as surface water became limited in quantity and quality. Assessment of the groundwater potential (GWP) in the basin is crucial for sustainable use of water resources. This study aims at assessing the GWP in the basin using remote sensing and GIS-based Multi Criteria Decision Analysis (MCDA). Seven factors (lithology, lineaments, drainage density, rainfall, slope, land use/land cover and soils) that affect groundwater distribution were considered. Analytical Hierarchy Process (AHP) approach were used to compute each layer weight. Thematic weighted layers were overlaid in ArcGIS to identify GWP are-as in the basin. The result indicated that, 15% (1765 km<sup>2</sup>) classified as “very high”, 26.5% (3151 km<sup>2</sup>) as “high”, 31% (3592 km<sup>2</sup>) as “medium”, and 27.5% (3224 km<sup>2</sup>) were classified as “low” GWP zones in the basin. The GWP map was validated using observed borehole and springs data in the basin, and it indicated that 76% of agreement. It was found that GWP was highly sensitive to lithology and rainfall with mean variation index of 2.7% and 2.0%, respectively. High GWP is available at the southern and eastern side of the Lake Tana.

**Keywords:** Groundwater · GIS and RS · Lake Tana · Blue Nile · Ethiopia

## 1 Introduction

Groundwater resource is an important natural resource for its use in agriculture, industries and domestic purposes. It is unevenly distributed both spatially and temporally all over the world. In northern Ethiopia, where rainfall is scarce and unevenly distributed; groundwater is the main source to meet various water demands [4]. The demand for groundwater in Lake Tana basin (LTB) has been increasing over the years [48]. Development of groundwater resources is essential to satisfy the increasing

demand [47]. In this area, groundwater recharge varies significantly in space and time due to the difference in distribution and amount of rainfall, permeability of rocks, geomorphology and availability of surface water bodies close to major unconfined and semi-confined aquifers that feed the groundwater [4–37].

There are several conventional methods, used to assess groundwater potential, some are: Ground surveys, Geophysical Methods such as resistivity, and ground penetrating radar; Probabilistic Models like Logistic Regression Methods [3] are unreliable and time consuming. There are also various statistical methods that were adopted for groundwater potential mapping such as frequency ratio [13–27], multi-criteria decision evaluation [16–43], weights-of-evidence model [29]; random forest model [24] maximum entropy model [30] boosted regression tree, classification and regression tree [24]. Remote sensing and Geographic Information System (GIS) techniques have become an easier, effective and time efficient in the assessment, monitoring and conservation of groundwater resources [45]. These days a number of researchers, [2, 10, 15, 19, 28] applied remote sensing and GIS through Analytical Hierarchy Process (AHP) for the assessment of groundwater potential.

Even though the importance of the groundwater resources is essential for development, limited groundwater studies have been carried out in the basin. The potential is not well defined. However, the government of Ethiopia has declared the Lake Tana – Beles as a growth corridor. Therefore, the objective of this study is to assess the groundwater potential in Lake Tana basin using Geographical Information System (GIS) and Remote Sensing (RS) based MCDA techniques, and to produce a groundwater potential map.

## 2 Methods and Materials

### 2.1 Description of the Study Area

Lake Tana basin is located in northwestern Ethiopia (Fig. 1), which feed to the Blue Nile River. Geographically, it is located between  $10^{\circ}57'$ – $12^{\circ}47'$ N and  $36^{\circ}38'$ – $38^{\circ}14'$ E. The basin landscape is part of the western plateau of Ethiopia and includes the escarpments of Gondar and Gojjam, the lower plains surrounding the lake that forms extensive wetlands of Dembiya, Fogera, and Kunzila plains located in the north, east, and southwest of the lake, respectively. The basin has a total area of 15,320 km<sup>2</sup>.

### 2.2 Data Collection and Preparation

In this study eight thematic layers (drainage density, rainfall, slope steepness, land cover/use, lineaments, soil and lithology) were used. The rainfall map was prepared using Inverse Distance Weighting (IDW) interpolation from 26 stations long term mean annual rainfall data. The lithology, soil, and land use are collected from Ethiopian Geological survey. These thematic layers were prepared using Arc GIS 10.1 platform. The drainage and lineament density maps have been prepared using the line density analysis tool in Arc GIS 10.1. The slope and drainage density were derived from

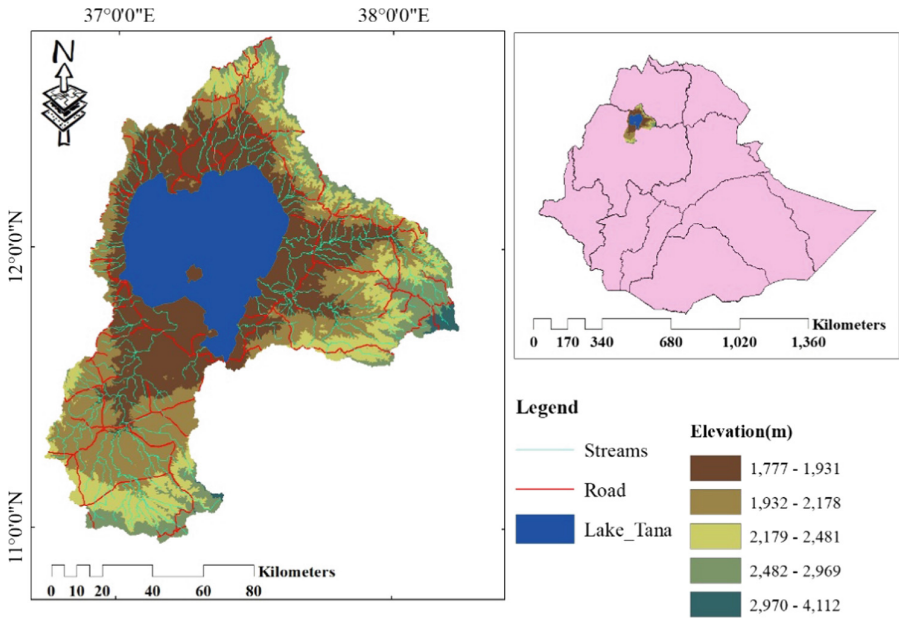


Fig. 1. Location map of Lake Tana basin

Shuttle Radar Terrain Mapping Digital Elevation Model (STRM DEM) of 30 m resolution. Arc Hydro tool was used to generate stream network and drainage density was calculated in Arc GIS 10.1 using Eq. 1 [12].

$$DD = \Sigma Li/A \tag{1}$$

Where, DD is drainage density; Li denotes the total length of streams (L) and A denotes the unit area.

Cloud free Landsat 8 Operational Land Imager (OLI) images (Row 52/Path 169, Row 51/Path 170, and Row 52/Path 170), dated June 17 and 24, 2017 were downloaded from USGS website (<https://earthexplorer.usgs.gov>) for lineament extraction. After applying principal component analysis (PCA) technique using ENVI 5.1 to produce uncorrelated output bands, to segregate noise components, and to reduce the dimensionality of data sets [25–43], lineaments were extracted automatically using PCI Geomatica 2017 trial version from Landsat 8 [23]. Lineament density was calculated in Arc GIS 10.1 using Eq. 2 [13].

$$LD = \Sigma Li/A \tag{2}$$

Where, LD is lineament density; Li is denotes the total length of lineaments (L) and A is denotes the unit area.

### 2.3 Weighting and Ranking of Each Layers (AHP)

Because all parameters do not have equal effect on groundwater distribution, ranking of each parameter is needed. Weighting each factor and a pair-wise comparison matrix were prepared for each map based on [34]. The rate/rank for classes in a layer and weights for each factor was assigned and a pair-wise comparison matrix has been prepared for each map by using Multi Criteria Decision Analysis technique based on Analytical Hierarchy Process (AHP) [35] by considering seven factors (lithology, lineament density, soil, and drainage, rainfall, slope and land use/cover). Square matrices are constructed, where each criterion is compared with the other criteria, relative to its importance, on Saaty’s scale from 1 to 9 (Table 2). The rate/rank for classes in a layer and weights for thematic layers of each factor was calculated as the following steps:

1. Square matrix  $A = a_{ij}$  (Eq. 3) the element of row  $i$  column  $j$  was produced and the lower triangular matrix was Completed by taking the reciprocal values of the upper diagonal using the formula  $a_{ij} = 1/a_{ji}$

$$A = \begin{pmatrix} \frac{p1}{P1} & \dots & \dots & \frac{P1}{Pj} & \dots & \dots & \frac{P1}{Pn} \\ \frac{Pj}{P1} & \dots & \dots & 1 & \dots & \dots & \frac{Pj}{Pn} \\ \frac{Pn}{P1} & \dots & \dots & \frac{Pn}{Pj} & \dots & \dots & 1 \end{pmatrix} \tag{3}$$

2. Summation of all columns  $j$  matrix from (Eq. 3) using (Eq. 4)

$$\frac{p1}{Pi} + \dots + \frac{Pi}{Pj} + \dots + \frac{Pn}{Pn} = (\sum_{i=1}^n Pi) / Pi \tag{4}$$

3. Divide each element of matrix  $a_{ij} = pi/pj$  (Eq. 3) by (Eq. 4) to get normalized relative weight (Eq. 5)

$$\frac{\frac{Pi}{Pj}}{(\sum_{i=1}^n Pi) / Pj} = \frac{Pi}{Pj} * \frac{Pj}{\sum_{i=1}^n Pi} = \frac{Pi}{\sum_{i=1}^n Pi} \tag{5}$$

4. Averaging across the rows (Eq. 6) to get the normalized principal Eigen vector (priority vector) i.e. Rate (Ri) or weight of row ‘i’(Wi). Since it is normalized, the sum of all elements in priority vector should be one.

$$Wi/Ri = \left( \frac{Pi}{\sum_{i=1}^n Pi} + \dots + \frac{Pi}{\sum_{i=1}^n Pi} \right) * 1/n \tag{6}$$

The judgments of the pair-wise comparison within each thematic layer were checked by the consistency ratio [35]. The consistency ratio (CR) is a measure of consistency of the pair-wise comparison matrix. Scholars [21–35] recommended that for matrices with CR rating greater than 0.1, the process is repeated until the desired value of CR < 0.1 is achieved. The value of CR is computed as (Eq. 7)

$$CR = CI/R \tag{7}$$

where, RI is Saaty’s ratio index; CI is Consistency index.

Consistency index is a measure of consistency or degree of consistency of the judgment [21–34] and computed using (Eq. 8).

$$CI = (\lambda_{max} - n)/(n - 1) \tag{8}$$

where, n is the number criterion, the value of RI for n criteria as indicated in Table 1.

**Table 1.** Random consistency index (RI)

Numbers of criteria (n)	Saaty’s ratio index (RI)
1	0
2	0
3	0.58
4	0.9
5	1.12
6	1.24
7	1.32
8	1.41
9	1.45

To compute  $\lambda_{max}$ , first multiply the normalized value by the respective Weight (Eq. 6) and then, the values of the product are added together to get  $\lambda_{max}$  (Eq. 9)

$$\lambda_{max} = \sum_{i=1}^n (Wi * (Pi / \sum_{i=1}^n Pi)) \tag{9}$$

where,  $\lambda_{max}$ , the largest Eigen value of the pair wise comparison matrix. Pi is the priority of the alternative and wi is the assigned rate/weight.

**Table 2.** Scale of preference between two parameters in AHP [34]

Scale	Degree of preference	Explanation
1	Equally	Two activities contribute equally to the objective
3	Moderately	The judgment slightly-to-moderately favor one activity
5	Strongly	The judgment strongly or essentially favor one activity
7	Very strongly	Very strong preference or importance
9	Extremely	Quite preferred or quite important
2, 4, 6, 8	Intermediate values	Preferences between the preferences in weights 1, 3, 5, 7 and 9

## 2.4 Overlay Analysis

After assigning the rates for classes in a layer and weights for thematic layers each factors the final map (Fig. 9) was obtained by overlaying all thematic maps using weighted overlay methods [19–21], using the spatial analysis tool in Arc GIS 10.1 as shown (Eq. 10)

$$GWP = \sum_{i=1}^n W_i * R_i \quad (10)$$

Where, GWP is groundwater potential zone;  $W_i$  is weight for each thematic layer and  $R_i$ ; rates for the classes within a thematic layer derived from AHP.

## 2.5 Sensitivity Analysis

The map-removal sensitivity analysis was used to examine the impacts of removing one of the thematic layers in the computation of the GWP distribution map. The map removal sensitivity analyses [5–17] were used to identify the factors that affect the groundwater potential, details are shown in Table 4. In this method, each of the thematic layers are removed, and a new GWP map is obtained each time for the remaining layers overlaying each other. Map removal shows the sensitivity of the GWP map to the removal of one of the thematic layers. This analysis is expressed in terms of an index of sensitivity as shown (Eq. 11).

$$S = [((GWP/N) - (GWP'/n))/GWP] * 100 \quad (11)$$

where  $S$  is the index of sensitivity associated with the removal of one map;  $GWP$  is the groundwater potential index computed using all the thematic layers;  $GWP'$  is the groundwater potential index computed by excluding one thematic layer at a time;  $N$  and  $n$  are the number of thematic layers used to compute  $GWP$  and  $GWP'$ , respectively.

# 3 Results and Discussion

## 3.1 Design and Preparation of Thematic Maps

### Drainage Density (DD)

Drainage Density is expressed as the total length of all streams or rivers per unit drainage area [12, 13]. In areas where a higher drainage density is dominant, groundwater potential is generally poor, because less time for infiltration. Whereas, areas of low drainage density allow more infiltration to recharge the groundwater system [1–22]. Stream network derived from 30 m DEM, mainly six drainage density categories have been identified and mapped as shown in Fig. 2. The highest drainage density was found in the southern, eastern and northeastern part of the Lake Tana basin. However, moderate and low drainage density concentrates in the southern and central

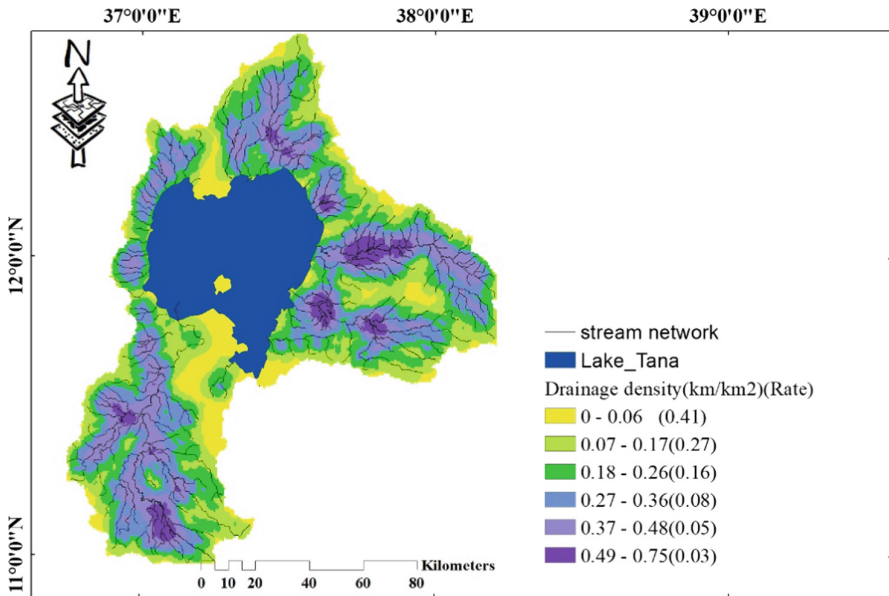


Fig. 2. Stream network and drainage density map of the Lake Tana basin

part of the lake basin. By using pairwise comparison, the rate was set based on groundwater potential for areas with low drainage density were assigned the higher rate, and high drainage density were assigned the lowest rate due to low groundwater potential. The lowest drainage density ( $0-0.06 \text{ km/km}^2$ ) were assigned the highest rate (0.41) and areas having higher drainage density  $0.35-0.5$  and  $0.5-0.8 \text{ km/km}^2$  were assigned the lowest rate of 0.05 and 0.03, respectively.

### Lineament Density (LD)

Lineaments are the simple and complex linear properties of geological structures like: faults, cleavages, fractures, and various surfaces of discontinuities (terraces and ridges) arranged in a straight line or a slight curve that are identified by remote sensing [25]. Lineaments were extracted automatically using Geomatica module, which is extracted from a single image of principal component analysis (PCA) and record the output as polyline with vector segment. Due to multispectral imaging bands are often highly correlated; Principal Components used to produce uncorrelated output bands, to segregate noise components, and to reduce the dimensionality of data sets [23–25]. This is done by finding a new set of orthogonal axes that have their origin at the data mean and that are rotated so the data variance is maximized. After applying Principal component analysis of Landsat images eight-bit gray scale lineaments are extracted automatically (Fig. 3). Areas with high lineament density are assumed good for groundwater potential [10–41]. From the result, the highest lineament density was observed in the North Eastern escarpments and South tip of the basin. As shown in Fig. 3, the highest lineament density ( $0.63-1.10 \text{ km/km}^2$ ) was assigned the maximum rank (0.39) and the lowest rate/rank (0.02) was assigned to the lineament density class of  $0-0.083$ .

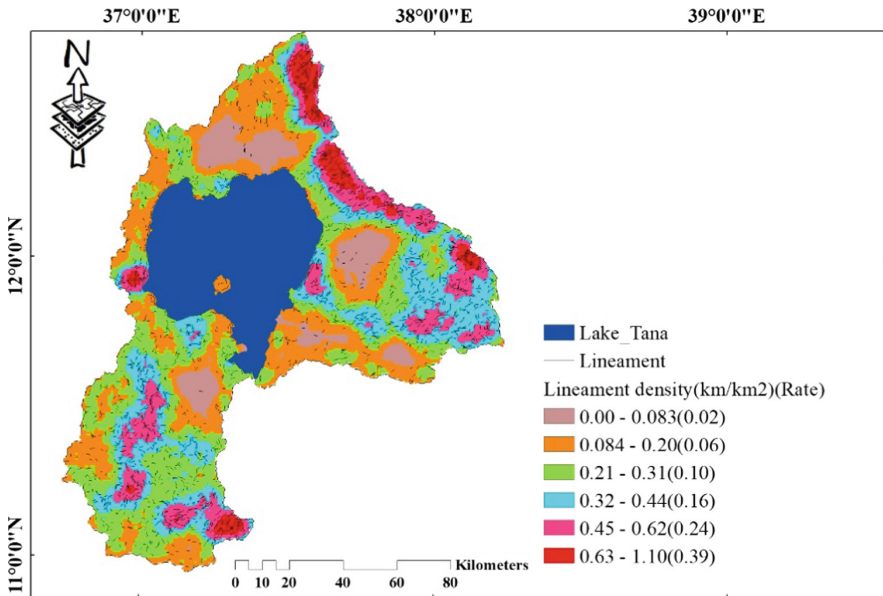


Fig. 3. Lineament density map

**Slope**

Slope defines the variation of elevation in a particular area which influences the runoff [24]. In gentle slopes, the movement of water is generally slow, which allows more infiltration. Whereas, in steep slopes runoff is favored and lower infiltration. Slope map has been derived from 30 m resolution DEM (Fig. 4). Slope varies from 0 to 72.8° and classified based on natural break classification method [26]. It classified in to six classes viz., 0–2.6, 2.6–6.7, 6.7–12.6, 12.6–19.4, 19.4–28.3, and 28.3–72.8. The highest rate (0.39) was assigned for the lowest slope gradient which is observed in central parts of the basin surrounding to Lake Tana and the lowest rate (0.02) was assigned for the highest slope gradient which found in northeastern, eastern and northern tip of the basin.

**Rainfall**

Rainfall is another factor that governs the amount of water that would be available to infiltrate and joins the groundwater zones, and thus it controls groundwater potential [42]. The rainfall map is classified into six classes using equal-interval classes [32]. Long term mean annual rainfall map of the area is prepared using IDW interpolation from 26 meteorological stations (Fig. 5). Based on the mean annual rainfall and its contribution for groundwater recharge; the relative weight (rate) was given for each rainfall classes. The rate was given based on the contribution to groundwater recharge, higher rate was assigned for high rainfall; and low rainfall areas were assigned the lowest rate for low groundwater potential [16]. Mean annual rainfall between 1713–2231 mm were assigned the highest rate (0.41), and 1507–1712 mm rainfall were assigned the next higher rate of 0.25. Areas having mean annual rainfall of 1039–1205 mm and less than 1000 mm mean annual rainfall were assigned the lowest rate as 0.05 and 0.03, respectively.



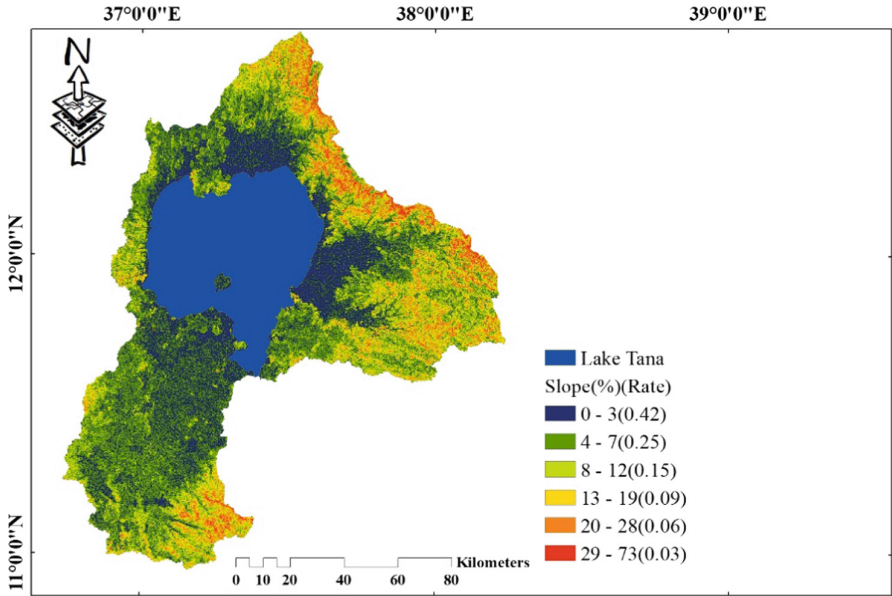


Fig. 4. Slope gradient of Lake Tana basin

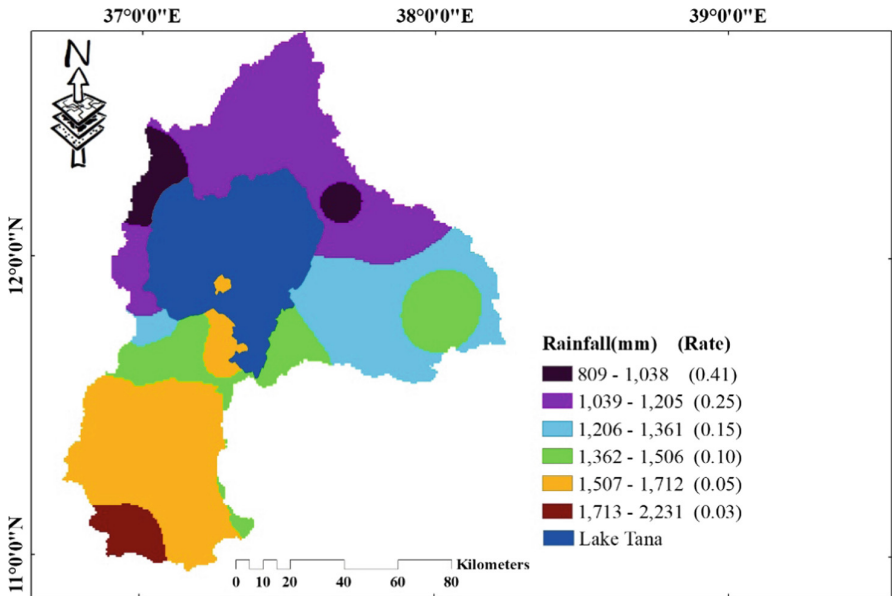
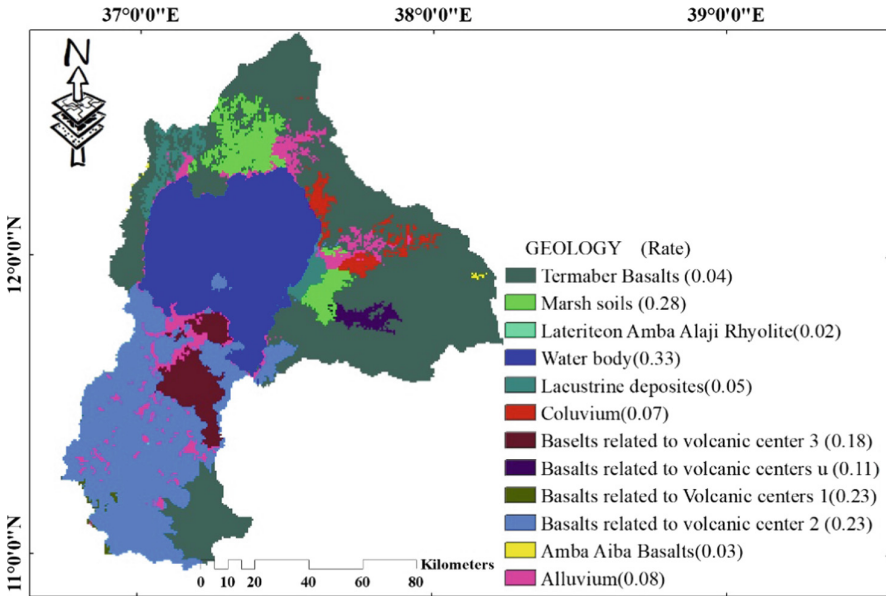


Fig. 5. Meteorological stations and rainfall map of Lake Tana basin

**Lithology**

Lithology plays an important role in the occurrence and distribution of groundwater. According to Ethiopian Geological survey, the major lithological units of Lake Tana basin are Tarmaber basalts (39.8%), Basalts related to volcanic center (26.5%), alluvium deposit (4.7%), lacustrine deposits (2.3%), colluvium (1.9%), Amba Aiba Basalts (0.07%), Lateriteon Amba Alaji Rhyolite (0.003%), marsh soil (4.7%), and Lake (20%). The basin covered by Basalts related to volcanic center mainly containing scoriaceous basalt widely found at southern part and the Tarmaber Basalts at northern, western and the southern end of the basin (6–7). The lowland covered by a thick Quaternary alluvial deposit (clay to gravel grain size), lacustrine deposits and Colluvium formed the major aquifer zones. Based on their age, the aquifer systems classified in to three major groups. Those are: the Tertiary Volcanic (Tarmaber formation, Amba Aiba Basalts and Lateriteon Amba Alaji Rhyolite), the Quaternary Fractured Vesicular Basalt (quaternary basalt related to volcanic centers) and the Quaternary Alluvial deposits such as Alluvium, Colluvium and Lacustrine deposits) [39, 40]. As shown as Fig. 6 the south part with Quaternary Basalt overlain by Alluvial Deposit displays the highest productive aquifer. However, the northern, southern and eastern mountainous regions, mostly covered by highly degraded tuff and massive basalt, are characterized by lowest productivity [40]. Thus, the highest rate was given for the highest productive aquifer, and the lowest rate was given for lowest productivity.



**Fig. 6.** Lithological map of Lake Tana basin (source: Ethiopian Geological survey)

**Land Use/Land Cover**

Land use cover significantly affects hydrological processes; i.e. interception, infiltration capacity of soil, runoff generation mechanism, are affected by the land use/land cover type. This in turn affect groundwater recharge and discharge [33]. Most of the study area is covered by cropland with sparse woodlands while only few limited areas of highlands are forested (less than 1% of the basin). The major land cover types are cropland 45%, wood land 18%, water body (20%), Grass land (13%), and bare land (2%) Forest (1%), and urban and built 0.2% [47]. As shown in Fig. 7 forests were assigned the highest rank due to less runoff because leaves and trees slow down the rain before it hits the ground, giving plant root’s time to infiltrate and join into the groundwater system. From the pair-wise comparison, the rate was given based on contributions for groundwater recharge [38]. Highest rates were assigned for areas cover with water bodies (0.26) and swampy (0.19). Whereas, the lowest rates were given for cultivated (0.02) and urban areas (0.01).

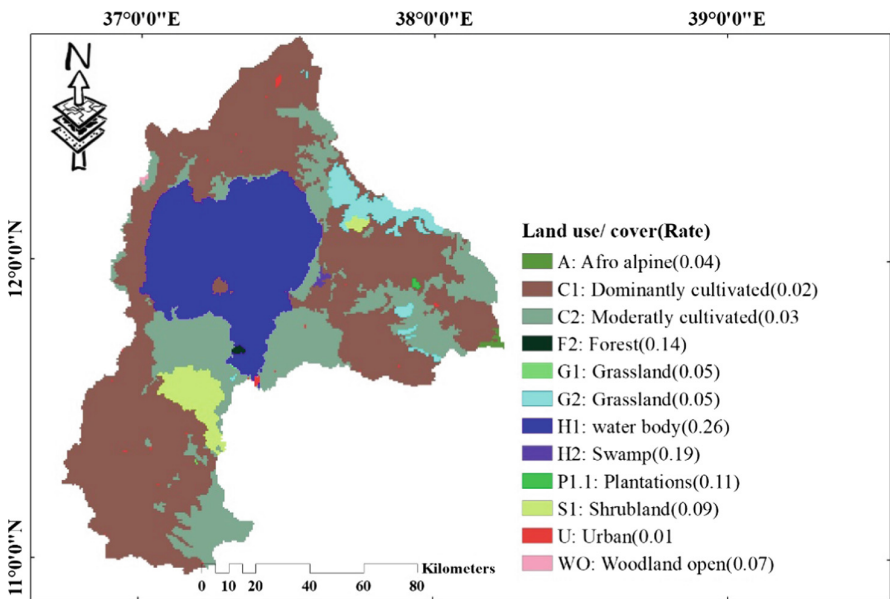


**Fig. 7.** Land use/land cover map of Lake Tana basin

**Soil Group**

Soil is an important factor for delineating the groundwater potential areas. Soil characteristics invariably control rates of infiltration; percolation and permeability [38–44]. Tana basin is covered by a wide range of soil groups. As shown Fig. 8, the major soils are: Haplic Luvisols which covers (26%), Chromic Luvisols (20%), Eutric Leptosols (16%), Eutric Vertisols (15%), Eutric Fluvisols (12%), Haplic Alisols (6%), Lithic Leptosols (3%), Haplic Nitisols as medium portion, and Eutric Regosols and Eutric Cambisols less than 1% of the basin. The southern part is covered by Haplic Luvisols

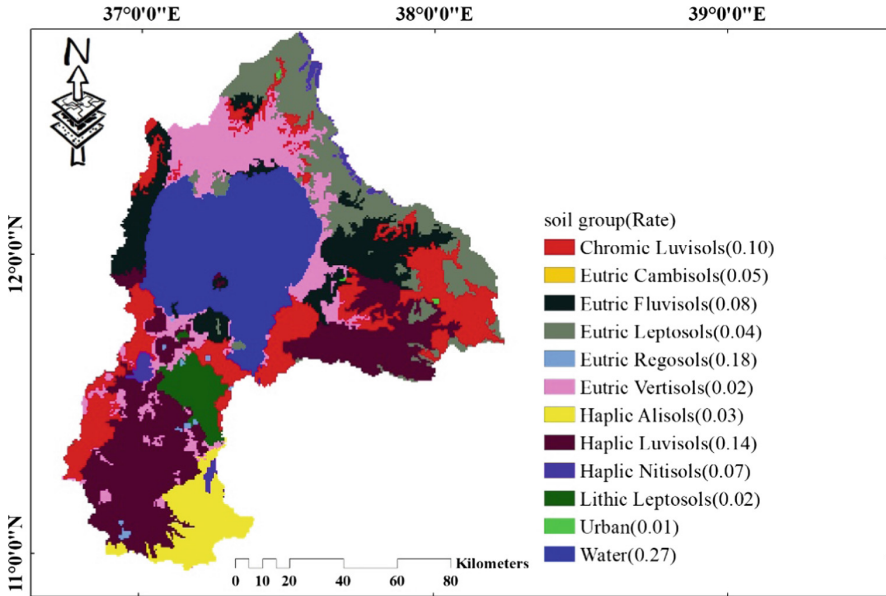


Fig. 8. Soil map of the Tana basin (source: Ethiopian Geological Survey)

and Chromic Livisols which have higher infiltration infers high groundwater potential [8]. The floodplain to the north and east of Lake Tana is covered by Eutric Leptosols and Eutric Vertisols which have the lowest infiltration rate. The major soil properties of Lake Tana basin are classified based on its texture, drainage condition and infiltration capacity. Thus, Eutric Regisols which are characterized by sandy loam to loam texture; It excessively drain and are categorized as soil group A as highly permeable and soil group B such as: Haplic Livisols, Chromic Livisols, Eutric Fluvisols and Haplic Nitisols are characterize as well drained to moderately drain condition due to having textural class of clay to silt clay [8]. Therefore, Eutric Regosols, Haplic Livisols and chromic Livisols which have higher infiltration were given the relative weight (rate) of 0.18, 0.14 and 0.10, respectively. However, soil group like Eutric vertisols and Lithic Leptosols which contain clay texture and characterized by poorly drained condition and assigned the lowest rate of 0.02 (Fig. 8).

### 3.2 Combination of Thematic Layers

Since for all layers, the value of consistency ratio (CR) is less than 0.1 and, hence, the judgments of the pair-wise comparison within each thematic layer (Table 3) were acceptable [35]. Therefore, groundwater potential areas were obtained by the combination of all layers using overlay analysis method in Arc GIS 10.1 [22] using Eq. (12).

$$GWPZ = 0.38 * LT + 0.24 * LD + 0.16 * Soil + 0.10 * SL + 0.06 * DD + 0.04 * RF + 0.02 * LU/C \tag{12}$$

**Table 3.** Pair-wise comparison matrix between all thematic layers (CR = 0.03)

Classes	GEO	LD	GM	SOIL	SL	DD	RF	LU	W
LT	1								0.38
LD	1/2	1							0.24
SOIL	1/4	1/2	1/2	1					0.16
SL	1/5	1/3	1/3	1/2	1				0.10
DD	1/6	1/5	1/4	1/2	1/2	1			0.06
RF	1/7	1/6	1/5	1/3	1/2	1/2	1		0.04
LU/C	1/9	1/7	1/6	1/5	1/4	1/3	1/2	1	0.02

where, W = Weight, LT = lithology, LD = lineament density, SL = slope, DD = drainage density, RF = rainfall, LU/C = land use/cover

As shown in Fig. 9, the southern and eastern part of the basin shows very high groundwater potential zones due to presence of Quaternary basalts related to volcanic centers which are highly productive, alluvial plain and gentle slope. Similar studies have been reported [18 36 & 38]. The least groundwater potential areas are found in south eastern and northern escarpments (tips) of study area. The result indicated that, about 15% (1765 km<sup>2</sup>) classified as “very high,” 26.5% (3151 km<sup>2</sup>) as “high,” 31% (3592 km<sup>2</sup>) as “medium,” and 27.5% (3224 km<sup>2</sup>) were classified as “low” groundwater potential areas in the basin.

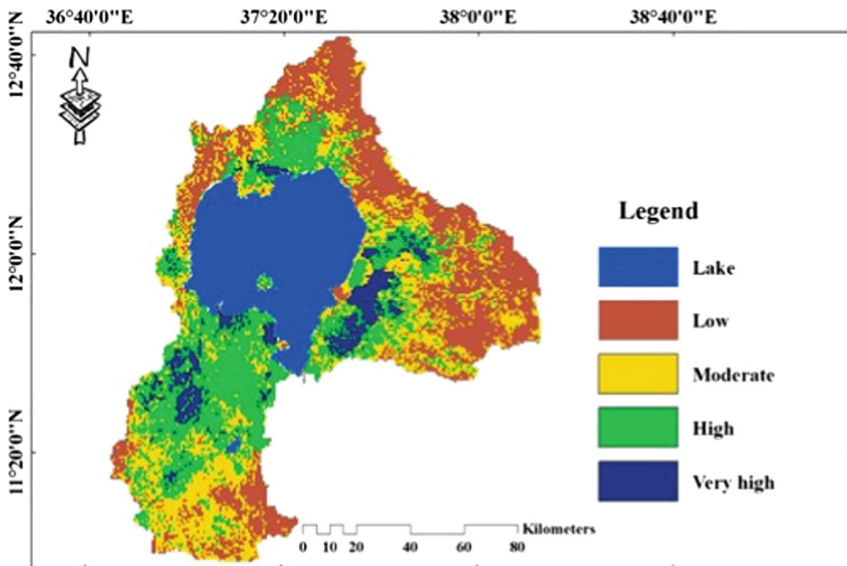


**Fig. 9.** Groundwater potential map of Lake Tana basin

### 3.3 Validation of Groundwater Potential Map

Validation of the groundwater potential zones were conducted using existing groundwater yield data of hand dug wells and/or bore holes and springs [9]. The groundwater potential map was verified with 195 existing boreholes and springs data (Fig. 10). Out of 195 existing water points (boreholes and springs) in which 149 (76%) were matched with its corresponding classes of groundwater potential zones (GWPZ). This indicates that, the groundwater potential map and actual borehole data shows good agreement.

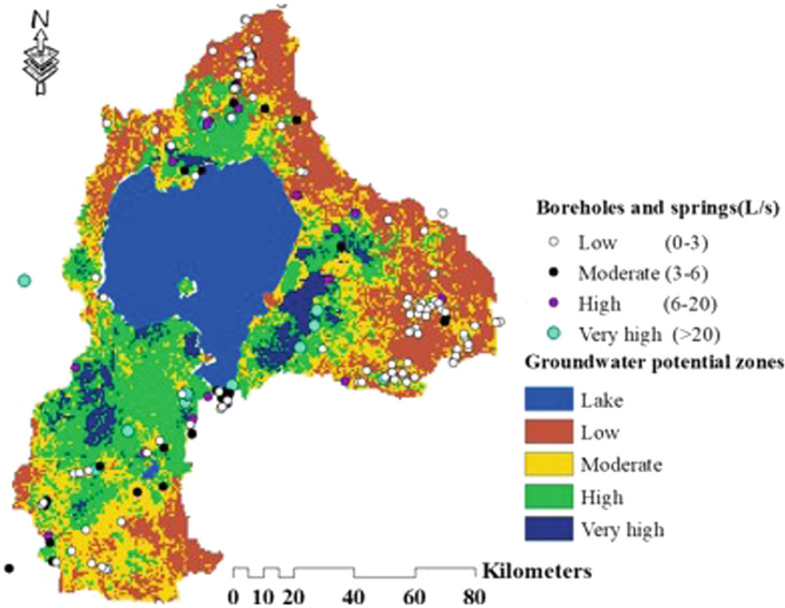


Fig. 10. Distribution of boreholes and springs with its yield in GWP zone

### 3.4 Sensitivity Analysis

Sensitivity analysis is important to know the influence of each factor on a ground-water potential map. For this study map removal, sensitivity analysis was used based on [5–17]. It indicates that the index variation of thematic layers by removing one thematic layer at a time using Eq. 6. As shown in the Table 4, the statistical summary of variation index resulting from removing each thematic layer was identified. The highest variation index with mean 2.65% associated to lithology, which is the highest sensitive parameter of groundwater potential. However, it is less sensitive to soil with mean variation index of 0.44%.

**Table 4.** Statistics of map removal sensitive analysis

Layer removed	Variation index (%)			
	Min	Max	Mean	SD
LT	0.75	3.14	2.70	3.79
LD	0.00	0.41	1.92	1.61
SOIL	0.40	0.45	0.44	0.46
SL	1.33	1.65	1.61	1.70
DD	0.00	0.77	0.89	2.99
RF	0.30	2.43	2.01	2.98
LU/C	1.53	1.58	1.53	1.52

where, Max = maximum,  
 Min = minimum, SD = standard  
 deviation, LT = lithology,  
 LD = lineament density,  
 GM = geomorphology, SL = slope,  
 DD = drainage density, RF = rainfall,  
 LU = land use/cover

## 4 Conclusions

The result of this study indicated that from the total area of the basin; about 27.5% (3224 km<sup>2</sup>) classified as: “low”, 30.6% (3592 km<sup>2</sup>) “moderate”, 26.9% (3151 km<sup>2</sup>) “high”, and 15% (1765 km<sup>2</sup>) “very high” groundwater potential zones, excluding the lake area. Out of 195 existing (borehole and springs) data for validation; 149 (76.4%) were agreed with corresponding groundwater potential classes. High ground-water potential was found at the southern and eastern side of Lake Tana. Groundwater can be exploited in these areas. On the other side, the least potential areas were found in northern, eastern and southern escarpments (tips) of the basin, respectively. This was because of the characterization by high gradient mountains, steep slope, high drainage density, hills, and hard-rock formation, which contribute high run off and less infiltration. Hence, in order to meet the increasing demand, new well fields may be formed in high groundwater potential zones, especially in the southern and eastern part of Lake Tana basin. But, in low groundwater areas, soil and water conservation measures and integrated watershed management should be applied to improve groundwater recharge. Future detail geophysical survey investigation in the basin is required for better results.

**Acknowledgments.** The authors would like to thank three anonymous reviewers for their constructive and insightful comments and suggestions which contributed improve the manuscript. The first author would like to provide his gratitude to: Bahir Dar University, Institute of Technology, University of Gondar and Ethiopian Road Authority (ERA) for sponsorship, Abay Basin Authority (ABA) and Amhara Design Works and Supervision Enterprise (ADWSE) are acknowledged for providing data.

## References

1. Agarwal, E., Agarwal, R., Garg, R.D., Garg, P.K.: Delineation of groundwater potential zone: an AHP/ANP approach. *J. Earth Syst. Sci.* **122**(3), 887–898 (2013)
2. Al-Abadi, A.M., Al-Shamma'a, A.: Groundwater potential mapping of the major aquifer in Northeastern Missan Governorate, South of Iraq by using analytical hierarchy process and GIS. *J. Environ. Earth Sci.* **10**, 125–149 (2014)
3. Alemayehu, T.: *Groundwater Occurrence in Ethiopia*, p. 107. Addis Ababa University, Addis Ababa (2006)
4. Al-Ruzouq, R., Shanableh, A., Merabtene, T.: Geomatics for mapping of ground-water potential zones in northern part of the United Arab Emirates - Sharjah City. In: *ISPRS - International Archives of the Photogrammetry, Remote Sensing and Spatial Information Sciences*, XL-7/W3, pp. 581–586 (2015). <https://doi.org/10.5194/isprsarchives-xl-7-w3-581-2015>
5. Babiker, I.S., Mohamed, M.A., Hiyama, T., Kato, K.: A GIS-based DRASTIC model for assessing aquifer vulnerability in Kakamigahara Heights, Gifu Prefecture, central Japan. *Sci. Total Environ.* **345**(1), 127–140 (2005)
6. BCEOM: *Abbay River Basin Integrated Development Master plan Project, Part-2, Hydrology* (1998)
7. Chorowicz, J., Collet, B., Bonavia, F.F., Mohr, P., Parrot, J.F., Korme, T.: The Tana basin, Ethiopia: intra-plateau uplift, rifting and subsidence. *Tectonophysics* **295**(3), 351–367 (1998)
8. Daniel, Y.: *Remote sensing based assessment of water resource potential for Lake Tana Basin*. M. Sc. thesis, Addis Ababa University (2007)
9. Fashae, O.A., Tijani, M.N., Talabi, A.O., Adedeji, O.I.: Delineation of groundwater potential zones in the crystalline basement terrain of SW-Nigeria: an integrated GIS and remote sensing approach. *Appl. Water Sci.* **4**(1), 19–38 (2014)
10. Fenta, A.A.: *Spatial analysis of groundwater potential using remote sensing and GIS-based multi-criteria evaluation in Raya Valley*. *Hydrogeol. J.* (2014). <https://doi.org/10.1007/s10040-014-1198-x>
11. Thannoun, R.G.: Automatic extraction and geospatial analysis of lineaments and their tectonic significance in some areas of Northern Iraq using remote sensing techniques and GIS. *Int. J. Enhanc. Res. Sci. Technol. Eng. Bull.* **2** (2013)
12. Greenbaum, D.: *Review of remote sensing applications to groundwater exploration in basement and regolith* (1985)
13. Guru, B., Seshan, K., Bera, S.: Frequency ratio model for groundwater potential mapping and its sustainable management in cold desert, India. *J. King Saud Univ. Sci.* **29**(3), 333–347 (2017)
14. Horton, R.E.: Drainage-basin characteristics. *Eos Trans. Am. Geo Phys. Union* **13**(1), 350–361 (1932)
15. Jaiswal, R.K., Mukherjee, S., Krishnamurthy, J., Saxena, R.: Role of remote sensing and GIS techniques for generation of groundwater prospect zones towards rural development—an approach. *Int. J. Remote Sens.* **24**(5), 993–1008 (2003)
16. Kumar, T., Gautam, A.K., Kumar, T.: Appraising the accuracy of GIS-based multi-criteria decision making technique for delineation of groundwater potential zones. *Water Resour. Manage* **28**(13), 4449–4466 (2014)
17. Lodwick, W.A., Monson, W., Svoboda, L.: Attribute error and sensitivity analysis of map operations in geographical information systems: suitability analysis. *Int. J. Geogr. Inf. Syst.* **4**(4), 413–428 (1990)



18. MacDonald, A.M., Calow, R.C., Nicol, A.L., Hope, B., Robins, N.S.: Ethiopia: water security and drought (2001)
19. Magesh, N.S., Chandrasekar, N., Soundranayagam, J.P.: Delineation of groundwater potential zones in Theni district, Tamil Nadu, using remote sensing, GIS and MIF techniques. *Geosci. Front.* **3**(2), 189–196 (2012)
20. Malczewski, J.: GIS and Multicriteria Decision Analysis. Wiley, New York (1999)
21. Malczewski, J.: GIS-based multicriteria decision analysis: a survey of the literature. *Int. J. Geogr. Inf. Sci.* **20**(7), 703–726 (2006)
22. Murasingh, S.: Analysis of groundwater potential zones using electrical resistivity, RS & GIS techniques in a typical mine area of Odisha (2014)
23. Hassan, M.A., Adhab, S.S.: Lineament automatic extraction analysis for Galal Badra river basin using Landsat 8 satellite image. *Iraqi J. Phys.* **12**(25), 44–55 (2014)
24. Naghibi, S.A., Pourghasemi, H.R., Dixon, B.: GIS-based groundwater potential mapping using boosted regression tree, classification and regression tree, and random forest machine learning models in Iran. *Environ. Monit. Assess.* **188**(1), 44 (2016)
25. O’Leary, D.W., Friedman, J.D., Pohn, H.A.: Lineament, linear, lineation: some proposed new standards for old terms. *Geol. Soc. Am. Bull.* **87**(10), 1463–1469 (1976)
26. Osaragi, T.: Classification methods for spatial data representation (2002)
27. Ozdemir, A.: GIS-based groundwater spring potential mapping in the Sultan Mountains (Konya, Turkey) using frequency ratio, weights of evidence and logistic regression methods and their comparison. *J. Hydrol.* **411**(3), 290–308 (2011)
28. Pinto, D., Shrestha, S., Babel, M.S., Ninsawat, S.: Delineation of groundwater potential zones in the Comoro watershed, Timor Leste using GIS, remote sensing and analytic hierarchy process (AHP) technique. *Appl. Water Sci.* **7**(1), 503–519 (2017)
29. Pourghasemi, H.R., Beheshtirad, M.: Assessment of a data-driven evidential belief function model and GIS for groundwater potential mapping in the Koohrang Watershed, Iran. *Geocarto Int.* **30**(6), 662–685 (2015)
30. Rahmati, O., Pourghasemi, H.R., Melesse, A.M.: Application of GIS-based data driven random forest and maximum entropy models for groundwater potential mapping: a case study at Mehran Region, Iran. *Catena* **137**, 360–372 (2016)
31. Richards, J.A.: Remote Sensing Digital Image Analysis: An Introduction, p. 240. Springer, Berlin (1999). <https://doi.org/10.1007/978-3-642-30062-2>
32. Rose, R.S.S., Krishnan, N.: Spatial analysis of groundwater potential using remote sensing and GIS in the Kanyakumari and Nambiyar basins, India. *J. Indian Soc. Remote Sens.* **37**(4), 681–692 (2009)
33. Roy, S., Sahu, A.S.: Investigation for potential groundwater recharge area over the Kunur river basin, Eastern India: an integrated approach with geosciences. *J. Geomat.* **9**(2), 165–177 (2015)
34. Saaty, T.L.: The Analytic Hierarchy Process: Planning, Priority Setting, Resource Allocation, p. 287. MacGraw-Hill, New York International Book Company, New York (1980)
35. Saaty, T.L.: How to make a decision: the analytic hierarchy process. *Eur. J. Oper. Res.* **48**(1), 9–26 (1990)
36. Sedrette, R.: Automatic extraction of lineaments from Landsat Etm+ images and their structural interpretation: case Study in Nefza region (North West of Tunisia). *J. Res. Environ. Earth Sci.* **04**(2016), 139–145 (2016)
37. Seifu, K.: Groundwater in Ethiopia. Springer Hydrogeology. Springer, Heidelberg (2013). [https://doi.org/10.1007/978-3-642-30391-3\\_2](https://doi.org/10.1007/978-3-642-30391-3_2)
38. Sisay, L.: Application of Remote Sensing and GIS for Groundwater Potential Zone Mapping in Northern Ada’a Plain (Modjo Catchment) (2007)

39. SMEC, IP.: Hydrological Study of The Tana-Beles Sub-Basins, part 1. Sub-basins Groundwater Investigation report (2007)
40. SOGREA: Consulting service for detailed groundwater investigation & monitoring in tana and Beles sub-basins stage 1 final report (unpublished), Volume II - Part 6: Hydrogeological Survey (2013)
41. Subagunasekar, M., Sashikkumar, M.C.: GIS for the assessment of the groundwater recharge potential zone in Karunkulam block, Thoothukudi district, Tamil Nadu, India. *Int. J. Curr. Sci.* **15**, 159–162 (2012)
42. Terzer, S., Wassenaar, L.I., Araguás-Araguás, L.J., Aggarwal, P.K.: Global isoscapes for  $[\delta] 18\text{O}$  and  $[\delta] 2\text{H}$  in precipitation: improved prediction using regionalized climatic regression models. *Hydrol. Earth Syst. Sci.* **17**(11), 4713 (2013)
43. Thannoun, R.G.: Automatic extraction and geospatial analysis of lineaments and their tectonic significance in some areas of Northern Iraq using remote sensing techniques and GIS. *Int. J. Enhanc. Res. Sci. Technol. Eng. Bull.* **2** (2013)
44. Thapa, R., Gupta, S., Guin, S., Kaur, H.: Assessment of groundwater potential zones using multi-influencing factor (MIF) and GIS: a case study from Birbhum district, West Bengal. *Appl. Water Sci.* **7**, 4117–4131 (2017)
45. Tiwari, A.K., Lavy, M., Amanzio, G., De Maio, M., Singh, P.K., Mahato, M.K.: Identification of artificial groundwater recharging zone using a GIS-based fuzzy logic approach: a case study in a coal mine area of the Damodar Valley, India. *Appl. Water Sci.* **7**, 4513–4524 (2017)
46. Waikar, M.L., Nilawar, A.P.: Identification of groundwater potential zone using remote sensing and GIS technique. *Int. J. Innov. Res. Sci. Eng. Technol.* **3**(5), 1264–1274 (2014)
47. Wale, A.: Hydrological Balance of Lake Tana Upper Blue Nile Basin, Ethiopia (2008)
48. Worqlul, A.W., Collick, A.S., Rossiter, D.G., Langan, S., Steenhuis, T.S.: Assessment of surface water irrigation potential in the Ethiopian highlands: The Lake Tana Basin. *CATENA* **129**, 76–85 (2015)